Detection of Constrained Unknown Beacon Signals of Terrestrial Transmitters and LEO Satellites with Application to Navigation

Mohammad Neinavaie*, Joe Khalife†, and Zaher M. Kassas*
* Department of Electrical & Computer Engineering; The Ohio State University, USA
† Department of Mechanical & Aerospace Engineering; University of California, Irvine, USA
{neinavaie.1@osu.edu, kalifej@uci.edu, zkassas@ieee.org}

***Abstract*—Detection of unknown beacons of signals of opportunity (SOPs), whether terrestrial or from low Earth orbit (LEO) satellites is considered. The abundance of SOPs promises an attractive alternative to global navigation satellite system (GNSS) signals. However, some specifications of ambient SOPs may not be available to the public. In this paper, a computationally efficient cognitive opportunistic navigation framework is proposed to (i) detect constrained unknown beacons and (ii) estimate their Doppler frequencies. Experimental results are presented demonstrating the efficacy of the proposed framework in successful detection and Doppler tracking for both terrestrial cdma2000 signals and Orbcomm LEO satellite signals.**

I. Introduction

Signals of opportunity (SOPs) have been considered as an alternative to global navigation satellite systems (GNSS) [1], [2]. While some SOPs openly publish their specifications (e.g., cellular signals are described in 3GPP standards [3]), other SOPs do not make such information publicly available (e.g., low Earth orbit (LEO) satellite signals [4]). This makes acquiring and tracking the latter SOPs impossible.

Cognitive opportunistic navigation addresses this challenge via blind estimation of signal characteristics [5]. Assuming that the SOP follows a standard modulation scheme (e.g., phase shift keying (PSK) or quadrature amplitude modulation (QAM)) and a standard multiple-access technique (e.g. code-division multiple access (CDMA) or orthogonal frequency-division multiplexing (OFDM)), a cognitive opportunistic navigation receiver recovers the unknown signal structure, to exploit the signal and produce a navigation solution. Most communication systems employ a synchronization beacon signal for timing and carrier offset recovery. For example, in cellular CDMA, pseudorandom noise (PN) sequences are used on the forward-link pilot channel for synchronization proposes [6]. Other examples are the primary synchronization signal (PSS) and secondary synchronization signal (SSS) in cellular long-term evolution (LTE) and 5G systems [7], [8]. While different broadband services may use the same modulation schemes, their underlying configuration and parameters could differ. For instance, the Globalstar satellite system supposedly uses similar protocol to the IS-95 and cdma2000 cellular CDMA system but with different PN sequences [6]. Although the Globalstar system is in lot of ways similar to the cdma2000 system, Globalstar satellite signals cannot be acquired without knowing the corresponding PN sequences [9]. Preliminary experiments for navigation with partially known signals were conducted in [10]–[13]. In [14], unknown Starlink satellite signals were exploited for navigation for the first time.

The detection problem of an unknown source in the presence of other interfering signals falls into the paradigm of *matched subspace detectors* [15]–[17]. In the detection problem of constrained beacons, the integer constraint of the beacon symbols in the matched subspace detectors leads to a class of integer least square problems [18], [19]. One example of a constrained beacon is the PN sequence in CDMA-based communication systems. A low computational complexity approach to estimate the beacon symbols is symbol-by-symbol estimation, which suffers from a poor performance in low signal-to-noise ratio (SNR) regimes. In [20], a symbol-by-symbol estimation scheme was considered to blindly estimate the symbols of the PN sequences of Galileo and Beidou satellites, and a 1.8 m high-gain antenna was used to accumulate enough signal power. The optimal algorithm proposed in [18], [19] can be used to solve the integer least squares problem with a *polynomial* computational complexity. The computational and hardware complexity of the integer least squares problem are two of the main challenges that should be addressed in a cognitive opportunistic navigation framework. This paper proposes a near optimal beacon detector with *linear* computational complexity for signals with integer constraint. First, low computational complexity algorithms are proposed to tackle two of the main challenges of opportunistic navigation: *blind beacon signal detection* and *blind Doppler estimation*. Second, experimental results are presented demonstrating the efficacy of the proposed framework in successful blind detection and Doppler estimation for both terrestrial cdma2000 signals and Orbcomm LEO satellite signals.

The rest of the paper is organized as follows. Section II overviews the cognitive opportunistic navigation framework and describes the signal model. Section III discusses the proposed beacon detection and blind Doppler estimation algorithms. Section IV presents experimental results. Concluding remarks are given in Section V.

This work was supported in part by the Office of Naval Research (ONR) under Grant N00014-22-1-2242 and in part under the Air Force Office of Scientific Research (AFOSR) under Grant FA9550-22-1-0476.

II. Cognitive Opportunistic Navigation and Baseband Signal Model

This section provides an overview of the cognitive opportunistic navigation framework and describes the baseband received signal model on which the framework operates.

A. Framework Overview

A *Cognitive opportunistic navigation* system mainly relies on blind detection and tracking of beacon signals in broadband communication systems, e.g., detecting the PN sequence in 3G cdma2000 systems or the SSS or PSS in 4G LTE and 5G systems [5]. From limited prior information about a particular broadband system, crucial unknown parameters along with the beacon or pilot signals are estimated, which in turn allows for exploiting received signals for navigation purposes.

A beacon or a pilot signal is a signal known by the receiver and is used for timing and carrier synchronization. Correlation-based receivers are typically used to detect the presence of beacon signals and synchronize to them. These receivers are typically capable of reliably detecting known beacon signals at relatively low SNRs. However, the beacon is unknown to a cognitive opportunistic receiver and the signal's SNR can be too low for reliable blind detection. As such, coherent integration becomes crucial to increase the effective SNR of the received beacon signal. To coherently integrate successive transmissions of the beacon signal, the Doppler shift (or Doppler frequency) must be estimated. Therefore, the two building blocks of a cognitive opportunistic navigation system are (i) blind Doppler estimation/tracking and (ii) blind beacon detection/tracking. Once a blind estimate of the Doppler is produced, one can perform coherent integration and feed the integrated signal to a detection algorithm to detect and estimate the symbols of the beacon sequence.

B. Received Baseband Signal Model

Let $s(t)$ denote the beacon signal consisting of N consecutive symbols with symbol duration T_{symb}. Each symbol is drawn from an arbitrary MPSK constellation. The beacon signal is continuously transmitted at a period of $N \cdot T_{\text{symb}}$. After channel propagation and baseband sampling at interval T_s, the received signal can be modeled as

$$y[n] = \sum_{i=-\infty}^{\infty} \alpha \exp\left(j2\pi\Delta f n\right) s[n - iL - n_d] + w[n], \quad (1)$$

where $y[n]$ is the complex baseband sample at the nth time slot; $L = N\frac{T_{\text{symb}}}{T_s}$ is the length of the beacon in samples; $\Delta f \triangleq f_D T_s$ is the normalized Doppler frequency and f_D is the true Doppler frequency in hertz; $w[n]$ models noise and interference; n_d is the unknown delay of the received beacon signal; and α is an unknown complex amplitude. For convenience of notation, define the kth truncated vector of received samples of length L as

$$\mathbf{y}^k \triangleq [y[kL], y[kL+1], \ldots, y[(k+1)L-1]]^T. \quad (2)$$

III. Detection of the Beacon Signal and Blind Doppler Estimation

Consider an observation vector $\mathbf{y}^k$ of length L. One can reformulate the system model as

$$\mathbf{y}^k = \alpha \mathbf{d}^k \odot \mathbf{s}^k + \mathbf{w}^k, \quad (3)$$

where α is the unknown complex amplitude of the received signal and is considered to be constant in the coherent processing interval, $\odot$ is the Hadamard product, $\mathbf{w}^k$ is an independent and identically distributed (iid) noise with zero mean and variance σ^2, and $\mathbf{d}^k$ captures the effect of the Doppler, i.e.,

$$\mathbf{d}^k = [\exp(j2\pi\Delta f(kL)), \ldots, \exp(j2\pi\Delta f((k+1)L-1)].$$

Also, consider the set $\mathcal{L}$ consisting all M^L vector combinations whose elements are the integers between 0 to $M-1$. For Mary PSK, a beacon sequence is $\mathbf{s}^k = \exp\left(\frac{j2\pi}{M}\mathbf{q}\right)$ where $\mathbf{q} \in \mathcal{L}$. The problem of non-coherent blind detection of $\mathbf{q}$ and Δf is addressed in the following subsection.

A. Beacon Signal Detection

One can show that the non-coherent maximum likelihood (ML) detector of $\mathbf{q}$ is

$$\left\{\hat{\mathbf{q}}, \hat{\Delta f}\right\} = \arg \max_{\mathbf{q}\in\mathcal{L}, \Delta f} \left| \left(\left(\mathbf{d}^k\right)^* \odot \mathbf{y}^k \right)^H \exp\left(\frac{j2\pi}{M}\mathbf{q}\right) \right|, \quad (4)$$

where $(\cdot)^*$ and $(\cdot)^H$ are the complex conjugate and Hermitian operators, respectively. For convenience, define $\mathbf{z} \triangleq \left(\mathbf{d}^k\right)^* \odot \mathbf{y}^k$. A solution to the optimization problem (4) consists of a linear search over Doppler candidates and an exponential brute-force search over all possible values of $\mathbf{q}$. Denoting the number of Doppler search candidates by $|D|$, the order of the overall search is $|D|M^K$. In an effort to solve (4) in less than quadratic complexity, a technique that has been utilized in [21], [22] will be adopted. The following lemma calculates the reduced number of search candidates.

Lemma 1: The optimal solution of the optimization problem (4) can be obtained by searching over $|D|L$ candidates.

Proof: In order to calculate the number of search candidates, first, rewrite the coherent detector of $\mathbf{q}$ for a given phase complex amplitude α. Note that the coherent detector does not depend on the magnitude of α, but only depends on its phase ϕ. More precisely, for a given value of ϕ, one has [21]

$$\left\{\mathbf{q}_\phi, \hat{\Delta f}\right\} = \arg \max_{\mathbf{q}, \Delta f} \Re\left\{ \exp(-j\phi)\mathbf{z}^H \exp\left(\frac{j2\pi}{M}\mathbf{q}\right) \right\}. \quad (5)$$

Due to the nature of iid noise and the independence of the elements of $\mathbf{s}^k$, the coherent detector simplifies to a symbol-by-symbol Mary PSK detector for a given Δf and ϕ. Hence, the kth element of $\mathbf{q}_\phi$ is obtained by mapping the phase of the kth element of $\exp(j\phi)\mathbf{z}$ to the closest multiple of $\frac{2\pi}{M}$, i.e.,

$$\mathbf{q}_\phi[k] = \text{round}\left[(\phi_k + \phi) \frac{M}{2\pi} \right] \mod M, \quad (6)$$

where mod is the modulus operator and $\phi_k \triangleq \arg\{\mathbf{z}[k]\}$. Thus, for a given Δf, one can find the optimal $\mathbf{q}$ by searching

over all possible values for ϕ. However, it can be readily shown from (6), that $\mathbf{q}_\phi$ and $\mathbf{q}_{\phi+\frac{2\pi}{M}}$ result in the same likelihood function in (4). Consequently, the search space for ϕ is limited to the interval $[0, \frac{2\pi}{M})$.

Since ϕ is limited to the interval $[0, \frac{2\pi}{M})$, a detected MPSK symbol will have an ambiguity of 2 instead of M. That is, a particular $\mathbf{q}_\phi[k]$ can take one of two values, based on which symbol in the MPSK constellation is closest to it. Define $\mathbf{c}_1 \triangleq \mathbf{q}_{\phi=0}$ and $\mathbf{c}_2 \triangleq \mathbf{q}_{\phi=\frac{2\pi}{M}}$, where it can be shown through (6) that $\mathbf{c}_2[k] = (\mathbf{c}_1[k]+1) \bmod M$. It can also be shown using (6) that the boundary angle between two symbols in the MPSK constellation is given by $\gamma_k \triangleq \frac{2\pi}{M}\mathbf{c}_1[k]+\frac{\pi}{M}-\phi_k$. Subsequently, each candidate MPSK symbol will be given by

$$\mathbf{q}_\phi[k] = \begin{cases} \mathbf{c}_1[k] & \phi \le \gamma_k, \\ \mathbf{c}_2[k] & \phi > \gamma_k. \end{cases} \tag{7}$$

For convenience of notation, sort the values of γ_k in an ascending order with a new index k' such that $\gamma_{k'+1} > \gamma_{k'}$. Therefore, the first boundary angle is $\gamma_{1'}$. Consequently, each candidate is of the form

$$[\mathbf{q}_{\phi=0}[1] + 1 - u(\gamma_1' - \phi), \ldots, \mathbf{q}_{\phi=0}[L] + 1 - u(\gamma_L' - \phi)]^T, \tag{8}$$

where $u(\cdot)$ is the unit step function. Equation (8) implies that for different values of ϕ, one has L different candidates $\mathcal{A} = \{\mathbf{a}_1, \ldots, \mathbf{a}_L\}$. Each candidate should be plugged in (4) to get the optimal $\hat{\mathbf{q}}$. Finally, by searching over Doppler the total number of $|D|L$ search candidates are obtained. ■

According to Lemma 1, in order to find the candidate effectively, one needs to solve

$$\left\{\hat{\mathbf{q}}, \hat{\Delta f}\right\} = \arg \max_{\mathbf{q}\in\mathcal{A}, \Delta f} \left| \left(\left(\mathbf{d}^k\right)^* \odot \mathbf{y}^k \right)^H \exp\left(\frac{j2\pi}{M}\mathbf{q}\right) \right|, \tag{9}$$

where $\mathrm{card}\,(\mathcal{A}) = |D|L$ and $\mathrm{card}(\mathcal{A})$ is the carnality of the set $\mathcal{A}$. Note that according the proof of lemma 1, by plugging the consecutive candidates $\mathbf{a}_l$ in (4), the following recursive formula is obtained, which can be used to solve (4) effectively,

$$\begin{aligned} \mathbf{z}^H \exp\left(\frac{j2\pi}{M}\mathbf{a}_l\right) &= \mathbf{z}^H \exp\left(\frac{j2\pi}{M}\mathbf{a}_{l-1}\right) \\ &+ \mathbf{z}[l]^* \exp\left(\frac{j2\pi}{M}\mathbf{a}_1[l]\right)\left(\exp\left(\frac{j2\pi}{M}\right) - 1\right). \end{aligned} \tag{10}$$

Equation (10) demonstrates the recursion between the likelihood functions corresponding to each candidate. It can be seen from (10) that the lth likelihood only depends on the lth observation and the previous likelihood. Therefore, a tree based algorithm based on (10) can be employed to optimally detect the beacon sequence with a computational complexity of order $|D|L$.

B. Blind Doppler Estimation

The performance of the beacon signal detection algorithm, and consequently the accuracy of the cognitive navigation system, depends on the effective SNR. It is essential to account for the Doppler in order to coherently integrate the observations and increase the effective SNR. A blind Doppler estimation (BDE) method is proposed, which is capable of estimating the Doppler even when the beacon sequence is unknown. The main idea of the BDE algorithm is performing a nonlinear operation to remove the beacon sequence from the observation vector and applying the least squares (LS) method to estimate the Doppler via the beacon-free observation. Let us express the actual normalized Doppler frequency as

$$\Delta f = \Delta f_{\mathrm{I}} + \Delta f_{\mathrm{D}}, \tag{11}$$

where $\Delta f_{\mathrm{I}} \triangleq \frac{m}{L}$ is referred to as the integer part and $\Delta f_{\mathrm{D}} \in [-\frac{1}{2L}, \frac{1}{2L}]$ is referred to as the decimal part of the Doppler. The nonlinear transformation $\left(\mathbf{y}^k\right)^M$, which raises each element of $\mathbf{y}^k$ to the power M, produces a term where the beacon sequence is wiped off. The LS estimate of Δf_{I}, denoted by $\hat{\Delta} f_{\mathrm{I}}$, boils down to the maximizer of the magnitude of the L point discrete Fourier transform (DFT) of $\left(\mathbf{y}^k\right)^M$ [23]. After wiping off the integer Doppler from the original observation, which results in the new observation vector $\mathbf{y}_{\mathrm{D}}^k$, the decimal part can be estimated by dividing the phase of the inner product $(\mathbf{y}_{\mathrm{D}}^k)^H \mathbf{y}_{\mathrm{D}}^{k+1}$ by the beacon period.

The details of the BDE method are presented in Algorithm 1. Note that in Algorithm 1, K is the coherent processing interval, i.e., the number of successive frames for which the Doppler frequency is assumed constant.

Algorithm 1: BDE algorithm

Input: $\mathbf{y}^k$ for $k = 1, \ldots, K$

Output: $\hat{\Delta} f_{\mathrm{I}}^k$ and $\hat{\Delta} f_{\mathrm{D}}^k$

1. Calculate $\hat{b}^k = \arg\max \left\{ \left| \mathrm{FFT}\left(\left(\mathbf{y}^k\right)^M \right) \right| \right\}$ for $k = 1, \ldots, K$.
2. Find $\hat{\Delta} f_{\mathrm{I}}^k = \begin{cases} \frac{\hat{b}^k}{ML} & \hat{b}^k \le \frac{L}{2} \\ \frac{L-\hat{b}^k}{ML} & \hat{b}^k > \frac{L}{2} \end{cases}$ and $\hat{\Delta} f_{\mathrm{I}} = \frac{1}{K}\sum_{k=1}^{K} \hat{\Delta} f_{\mathrm{I}}^k$.
3. Wipe-off the integer part as $\mathbf{y}_D^k = [\exp(-j2\pi\hat{\Delta} f_{\mathrm{I}}(kL)), \ldots, \exp(-j2\pi\hat{\Delta} f_{\mathrm{I}}((k+1)L-1)]\mathbf{y}^k$.
4. Find the decimal part as $\hat{\Delta} f_{\mathrm{D}}^k = \frac{1}{2\pi L}\arg\left\{(\mathbf{y}_D^k)^H \mathbf{y}_D^{k+1}\right\}$ and calculate $\hat{\Delta} f_{\mathrm{D}} = \frac{1}{K}\sum_{k=1}^{K-1} \hat{\Delta} f_{\mathrm{D}}^k$

IV. Experimental Results

A. Experiment 1: cdma2000 signals

This section presents experimental results for UAV navigation with real cdma2000 signals, uisng the proposed cognitive opportunistic navigation framework.

1) Experimental Setup: A UAV was equipped with an Ettus E312 universal software radio peripheral (USRP) to sample cdma2000 signals, a consumer-grade 800/1900 megahertz cellular antenna, and a small consumer-grade GPS antenna to discipline the on-board oscillator. The receiver was tuned to a 882.75 megahertz carrier frequency, which is a cdma2000 channel allocated for the U.S. cellular provider Verizon Wireless. Samples of the received signals were stored for off-line

post-processing. The ground-truth reference for the UAV trajectory was taken from its on-board navigation system, which uses GPS, an inertial measurement unit (IMU), and other sensors. The UAV's total traversed trajectory was 1.72 km, which was completed in 3 minutes. Over this trajectory, the receiver on-board the UAV was listening to 4 base transceiver stations (BTSs), whose positions were mapped prior to the experiment. The experimental environment is shown in Fig. 1.

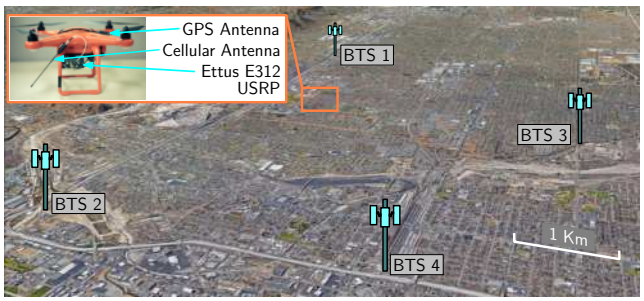

Fig. 1. Experimental setup and environment.

2) PN Sequence Detection Results: Next, the cdma2000 PN sequence is estimated from the forward link signal, as discussed in Section III. A scatter plot of the detected sequence is shown in Fig. 2(a), which seems to be very noisy even though a diamond shape is visible. Fig. 2(b) shows the correlation function between the detected and true cdma2000 forward channel PN sequence, whose clean peak indicates that the detected sequence can be reliably used to despread the cdma2000 signal. The detected PN sequence is then used to acquire and track the cdma2000 signals and produce carrier phase observables using the receiver implementation discussed in [24]. The carrier phase, expressed in meters, gives a measure of the distance between the transmitter and the receiver, up to a certain ambiguity [25]. In order to illustrate the ranging performance with the detected PN sequence, the change in distance with respect to the initial distance, called the delta range, was computed in two ways for each BTS: (i) using the UAV's and BTSs' known positions and (ii) from the carrier phase observables obtained with the detected PN sequence. The results are shown in Fig. 3.

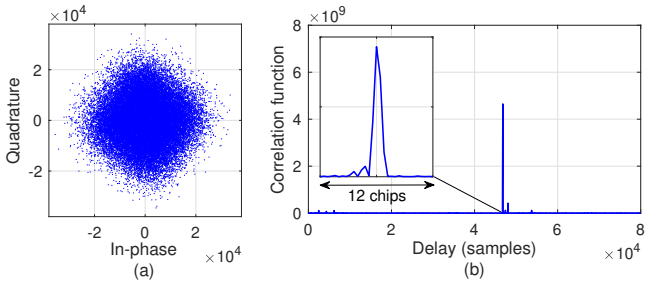

Fig. 2. (a) Scatter plot of the detected PN sequence from real cdma2000 forward channel signals. (b) Correlation function between the detected and true cdma2000 PN sequence.

3) Navigation Results: The single-receiver navigation framework developed in [26] was used to produce a navigation solution using the carrier phase measurements from the 4 BTSs. The total position root mean-square error (RMSE) was found to be 74.97 cm over the entire trajectory. The true and estimated trajectories are shown in Fig. 4.

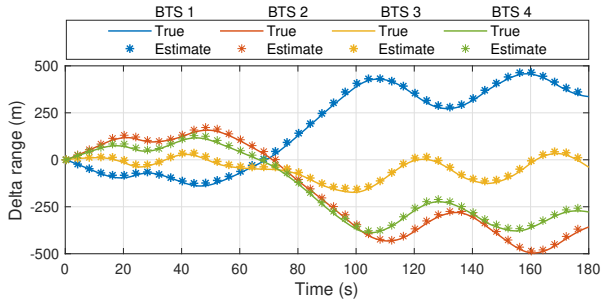

Fig. 3. Delta ranges in meters of the 4 BTS computed in two ways: (i) using the UAV's and BTSs' known positions (true) and (ii) from the carrier phase observables obtained with the detected PN sequence (estimate).

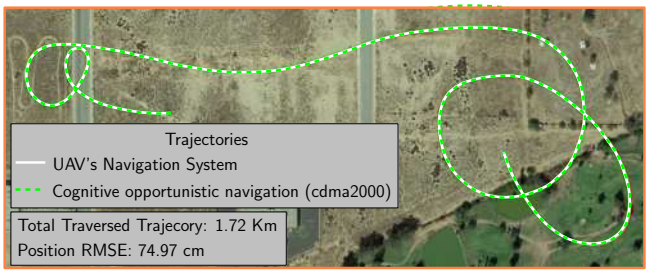

Fig. 4. True UAV trajectory and the estimated trajectory using the proposed cognitive opportunistic navigation framework.

B. Experiment 2: Orbcomm Satellite Signals

This section presents experimental results with Orbcomm LEO satellites on a stationary receiver.

1) Experimental Setup: A stationary receiver was equipped with an Ettus E312 USRP, a very high frequency (VHF) antenna, and a consumer-grade GPS antenna to discipline the on-board oscillator. The receiver was tuned to a 137 MHz carrier frequency with 2.4 MHz sampling bandwidth, which covers the 137–138 MHz band allocated to Orbcomm satellites. The LEO carrier phase measurements were produced at a rate of 4.8 kHz and were downsampled to 10 Hz. Over the course of the experiment, the receiver was listening to 2 Orbcomm satellites, namely FM 108 and FM 116.

2) Beacon Detection and Doppler Tracking Results: Unlike OFDM and CDMA-based signals where the signal power per degree of freedom is small, in classic modulation schemes, e.g., Mary PSK, a relatively larger power is dedicated to each degree of freedom. In other words, the allocated signal power per each time/frequency unit is relatively higher than spread spectrum techniques [27]. The Orbcomm constellation utilizes the classic symmetric differential phase shift keying (SDPSK) as the modulation scheme for downlink signals [28]. SDPSK is defined by a "zero" data state causing $-\frac{\pi}{2}$ phase shift and the "one" data state causing $+\frac{\pi}{2}$ phase shift. In order to increase the effective power of the periodic beacon in the Orbcomm constellation, the observation samples are raised to the power-of two, which turns the SDPSK modulated signal into a fixed sequence of binary samples, which is considered as the

reference signal for the proposed receiver. Fig. 5(a) shows the beacon signals of Orbcomm satellite signals. Fig. 5(b) shows the correlation function between the detected beacon signal of the Orbcomm satellite signals with the received signal, whose clean peak indicates that the detected beacon can be reliably used to despread the downlink signal. Fig. 6 compares Doppler tracking results of the two Orbcomm satellites using the proposed method versus the estimated Doppler from two-line element (TLE) files and an SGP4 propagator.

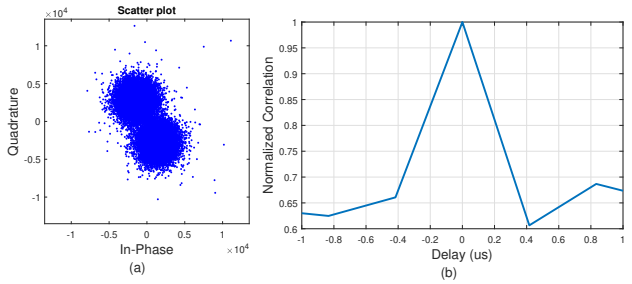

Fig. 5. (a) Scatter plot of detected beacon signals from Orbcomm satellite. (b) Correlation function between the detected beacon signal and received signal.

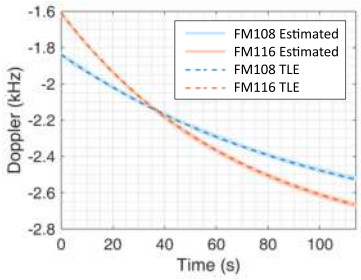

Fig. 6. Estimated Doppler from two Orbcomm LEO satellites versus the estimated Doppler from TLE files and SGP4 propagator.

V. Conclusion

This paper proposed a cognitive opportunistic navigation framework for constrained beacon signals. First, a low complexity blind detection algorithm was proposed to detect the beacon signal. Second, a blind algorithm was proposed to estimate the unknown Doppler frequency. The proposed framework was demonstrated with (i) cdma2000 signals, achieving submeter-accurate UAV navigation over a a 1.72 km trajectory and (ii) two Orbcomm LEO satellites, achieving beacon signal detection and Doppler tracking with a stationary receiver.

References

[1] J. Raquet *et al.*, "Position, navigation, and timing technologies in the 21st century," J. Morton, F. van Diggelen, J. Spilker, Jr., and B. Parkinson, Eds. Wiley-IEEE, 2021, vol. 2, Part D: Position, Navigation, and Timing Using Radio Signals-of-Opportunity, ch. 35–43, pp. 1115–1412.

[2] N. Souli, P. Kolios, and G. Ellinas, "Online relative positioning of autonomous vehicles using signals of opportunity," *IEEE Transactions on Intelligent Vehicles*, pp. 1–1, 2021.

[3] P. Wang and Y. Morton, "Carrier phase tracking architecture for positioning in LTE networks under channel fading conditions," in *Proceedings of ION GNSS+ Conference*, 2020, pp. 2605–2617.

[4] J. Khalife, M. Neinavaie, and Z. Kassas, "Blind Doppler tracking from OFDM signals transmitted by broadband LEO satellites," in *Proceedings of IEEE Vehicular Technology Conference*, April 2021, pp. 1–6.

[5] M. Neinavaie, J. Khalife, and Z. Kassas, "Cognitive opportunistic navigation in private networks with 5G signals and beyond," *IEEE Journal of Selected Topics in Signal Processing*, vol. 16, no. 1, pp. 129–143, 2022.

[6] L. Schiff and A. Chockalingam, "Signal design and system operation of Globalstar TM versus IS-95 CDMA – Similarities and differences," *Wireless Networks*, vol. 6, no. 1, pp. 47–57, February 2000.

[7] P. Wang and Y. Morton, "Performance comparison of time-of-arrival estimation techniques for LTE signals in realistic multipath propagation channels," *NAVIGATION, Journal of the Institute of Navigation*, vol. 67, no. 4, pp. 691–712, December 2020.

[8] A. Abdallah and Z. Kassas, "UAV navigation with 5G carrier phase measurements," in *Proceedings of ION GNSS Conference*, September 2021, pp. 3294–3306.

[9] R. Hendrickson, "Globalstar for the military," in *Proceedings of IEEE Military Communications Conference*, vol. 3, November 1997, pp. 1173–1178.

[10] J. Merwe, S. Bartl, C. O'Driscoll, A. Rügamer, F. Förster, P. Berglez, A. Popugaev, and W. Felber, "GNSS sequence extraction and reuse for navigation," in *Proceedings of ION GNSS+ Conference*, 2020, pp. 2731–2747.

[11] M. Neinavaie, J. Khalife, and Z. Kassas, "Blind opportunistic navigation: Cognitive deciphering of partially known signals of opportunity," in *Proceedings of ION GNSS Conference*, September 2020, pp. 2748–2757.

[12] M. Neinavaie, J. Khalife, and Z. Kassas, "Blind Doppler tracking and beacon detection for opportunistic navigation with LEO satellite signals," in *Proceedings of IEEE Aerospace Conference*, March 2021, pp. 1–8.

[13] M. Neinavaie, J. Khalife, and Z. Kassas, "Doppler stretch estimation with application to tracking Globalstar satellite signals," in *Proceedings of IEEE Military Communications Conference*, November 2021, pp. 647–651.

[14] Z. Kassas, M. Neinavaie, J. Khalife, N. Khairallah, J. Haidar-Ahmad, S. Kozhaya, and Z. Shadram, "Enter LEO on the GNSS stage: Navigation with Starlink satellites," *Inside GNSS Magazine*, vol. 16, no. 6, pp. 42–51, 2021.

[15] L. Scharf and B. Friedlander, "Matched subspace detectors," *IEEE Transactions on signal processing*, vol. 42, no. 8, pp. 2146–2157, 1994.

[16] A. Zaimbashi, M. Derakhtian, and A. Sheikhi, "GLRT-based CFAR detection in passive bistatic radar," *IEEE Transactions on Aerospace and Electronic Systems*, vol. 49, no. 1, pp. 134–159, 2013.

[17] A. Combernoux, F. Pascal, and G. Ginolhac, "Performance of the low-rank adaptive normalized matched filter test under a large dimension regime," *IEEE Transactions on Aerospace and Electronic Systems*, vol. 55, no. 1, pp. 459–468, 2019.

[18] G. Karystinos and D. Pados, "Rank-2-optimal adaptive design of binary spreading codes," *IEEE Transactions on Information Theory*, vol. 53, no. 9, pp. 3075–3080, 2007.

[19] P. Markopoulos and G. Karystinos, "Noncoherent Alamouti phase-shift keying with full-rate encoding and polynomial-complexity maximum-likelihood decoding," *IEEE Transactions on Wireless Communications*, vol. 16, no. 10, pp. 6688–6697, 2017.

[20] G. Gao, "Towards navigation based on 120 satellites: Analyzing the new signals," Ph.D. dissertation, Stanford University, 2008.

[21] K. Mackenthun, "A fast algorithm for multiple-symbol differential detection of MPSK," *IEEE Transactions on Communications*, vol. 42, no. 234, pp. 1471–1474, February 1994.

[22] W. Sweldens, "Fast block noncoherent decoding," *IEEE Communications Letters*, vol. 5, no. 4, pp. 132–134, April 2001.

[23] S. Kay, *Fundamentals of Statistical Signal Processing: Estimation Theory*. Prentice-Hall, Upper Saddle River, NJ, 1993, vol. I.

[24] J. Khalife, K. Shamaei, and Z. Kassas, "Navigation with cellular CDMA signals – part I: Signal modeling and software-defined receiver design," *IEEE Transactions on Signal Processing*, vol. 66, no. 8, pp. 2191–2203, April 2018.

[25] P. Misra and P. Enge, *Global Positioning System: Signals, Measurements, and Performance*, 2nd ed. Ganga-Jamuna Press, 2010.

[26] J. Khalife and Z. Kassas, "On the achievability of submeter-accurate UAV navigation with cellular signals exploiting loose network synchronization," *IEEE Transactions on Aerospace and Electronic Systems*, 2022, accepted.

[27] D. Tse and P. Viswanath, *Fundamentals of wireless communication*. Cambridge university press, 2005.

[28] S. Reid, "ORBCOMM system overview," December 2001.